MICROMACHINED STIMULATING ELECTRODES

Quarterly Report #11

(Contract NIH-NINDS-N01-NS-2-2379)

April 1995 --- June 1995

Submitted to the

Neural Prosthesis Program
National Institute of Neurological Disorders and Stroke
National Institutes of Health

by the

Center for Integrated Sensors and Circuits
Department of Electrical Engineering and Computer Science
University of Michigan
Ann Arbor, Michigan
48109-2122

July 1995

MICROMACHINED STIMULATING ELECTRODES

Summary

During the past quarter, work under this contract has been peformed in several areas. We have continued to fabricate passive probes for both internal and external users and are currently in the process of completing probes from four different mask sets. We are using the new site techniques described in the last quarterly report and have seen no further evidence of iridium adhesion problems. During the quarter, a number of chronic stimulation experiments were also completed. Electrode and tissue impedance, access resistance, and cyclic voltammetry data were taken throughout a week of stimulation on animals for two different current flow conditions. The chronic stimulating electrodes were implanted in the occipital lobe of an adult guinea pig. After a 10 day rest period, the stimulation protocol began. Site sizes of 1600μm^2 and 1000μm^2 were used. Each bipolar pair was stimulated for 4 hours a day for five days. The stimulus waveform was a biphasic pulse of 50μA magnitude, 0.1 msec/phase duration, and 250Hz rate. A 0.6V bias with respect to the reference was placed on the sites in between pulses. The electrical parameters of the electrode tissue system remained fairly constant during the measurement period for both along-shank and between-shank stimulation, indicating no significant changes in either the electrode properties or the tissue near the electrode as the result of stimulation. In addition to these tests, a long-term in-vitro pulse experiment was begun in PBS with parameters similar to those used in-vivo. The probe used in this test was fabricated with the new metalization protocol. To date, approximately 160 million pulses have been applied to the electrode sites. After an initial drop in impedance during the first day of testing, no significant subsequent changes have been seen.

Additional tests have been performed in-vitro and in-vivo using active probes realized from the most recent fabrication run. The monopolar probe, STIM-1b, functions well at frequencies up to 10MHz and has been used in additional experiments to stimulate in cochlear nucleus of the guinea pig while a silicon recording probe monitored the resulting driven single-unit activity in inferior colliculus (IC). As the site of stimulation was changed over the active probe, the patterns of single-unit activity in the IC have been seen to change accordingly. While preliminary in nature, these experiments mark the first successful use of an active probe in tissue. STIM-1a, an active bipolar probe, has also been characterized further in-vitro. The background bias current on both the positive and negative supplies is about 20μA, which is very close to the level expected. The current sourced by this probe is a linear function of the DAC setting over the full 0 to 127μA output range as expected. However, the negative sink current is linear only up to about 80μA, above which it has a weaker dependence on the DAC setting. The reason for this nonlinearity is being investigated but the problem should not preclude use of the probe at lower current levels. A weakness in the ability of STIM-2, the multipolar probe, to sink high currents has also been observed as noted in the previous report. By adjusting the supply voltages, however, this device can sink currents of over 60μA at frequencies of up to 400kHz. This is high enough to allow the use of STIM-2 in many in-vivo experiments, where additional experience using the probe will be gained during coming months. Needed changes will then be made to the probe design so that all observed problems can be corrected in a single design/process iteration later this year.

MICROMACHINED STIMULATING ELECTRODES

1. Introduction

The goal of this research is the development of active multichannel arrays of stimulating electrodes suitable for studies of neural information processing at the cellular level and for a variety of closed-loop neural prostheses. The probes should be able to enter neural tissue with minimal disturbance to the neural networks there and deliver highly-controlled (spatially and temporally) charge waveforms to the tissue on a chronic basis. The probes consist of several thin-film conductors supported on a micromachined silicon substrate and insulated from it and from the surrounding electrolyte by silicon dioxide and silicon nitride dielectric films. The stimulating sites are activated iridium, defined photolithographically using a lift-off process. Passive probes having a variety of site sizes and shank configurations have been fabricated successfully and distributed to a number of research organizations nationally for evaluation in many different research preparations. For chronic use, the biggest problem associated with these passive probes concerns their leads, which must interface the probe to the outside world. Even using silicon-substrate ribbon cables, the number of allowable interconnects is necessarily limited, and yet a great many stimulating sites are ultimately desirable in order to achieve high spatial localization of the stimulus currents.

The integration of signal processing electronics on the rear of the probe substrate (creating an "active" probe) allows the use of serial digital input data which can be demultiplexed on the probe to provide access to a large number of stimulating sites. Our goal in this area of the program has been to develop a family of active probes capable of chronic implantation in tissue. For such probes, the digital input data must be translated on the probe into per-channel current amplitudes which are then applied to the tissue through the sites. Such probes require five external leads, virtually independent of the number of sites used. As discussed in our previous reports, we are now developing a series of three active probes containing CMOS signal processing electronics. Two of these probes are slightly redesigned versions of an earlier first-generation set of designs and are designated as STIM-1a and STIM-1b. The third probe, STIM-2, is a second-generation version of our high-end first-generation design, STIM-1. All three probes provide 8-bit resolution in setting the per-channel current amplitudes. STIM-1A and -1B offer a biphasic range using ±5V supplies from 0μA to ±254μA with a resolution of 2μA, while STIM-2 has a range from 0 to ±127μA with a resolution of 1μA. STIM-2 offers the ability to select 8 of 64 electrode sites and to drive these sites independently and in parallel, while -1a allows only 2 of 16 sites to be active at a time (bipolar operation). STIM-1b is a monopolar probe, which allows the user to guide an externally-provided current to any one of 16 sites as selected by the digital input address. The high-end STIM-2 contains provisions for numerous safety checks and for features such as remote impedance testing in addition to its normal operating modes. It also offers the option of being able to record from any one of the selected sites in addition to stimulation.

During the past quarter, we have continued to fabricate passive probe structures using our new site formation techniques. No further problems with iridium adhesion have been experienced. A series of chronic stimulation experiments have been performed in-vivo to study electrode characteristics and the electrode-tissue system. Over a week of the experimental protocol, the electrical parameters of this system have remained nearly constant. Long-term pulse tests of the iridium electrodes have also been undertaken in PBS. In addition, further tests in-vitro and in-vivo with the active probes (STIM-1a, -1b, and -2) were carried out. The results in each of these areas are described below.

2. *Passive Probe Fabrication*

During the past quarter, we have continued to fabricate passive probes for both internal and external users. Since our fabrication facility is going our of operation for 2-3 weeks for maintenance on the air-handling equipment, it is important that the associated wafers be finished in the next two weeks. This includes stimulating as well as recording probes from four different mask sets. We are using the new site techniques described in the last quarterly report and have seen no further evidence of iridium adhesion problems with this process. Details of these passive probes have been given in the report on Recording Electrodes for the same time period (April through June 1995) and will not be repeated here.

3. *In-Vivo Current Flow and Impedance Studies*

This past quarter, a number of chronic stimulation experiments were completed. Electrode and tissue impedance, access resistance, and cyclic voltammetry data were taken throughout a week of stimulation on animals for two different current flow conditions. In addition, long-term *in vitro* pulse testing was begun to test iridium stimulating sites fabricated with the new metalization protocol (not the new site structure).

The goal of the chronic stimulation experiments is to measure the electrical parameters of the electrode-tissue system under conditions of bipolar and monopolar stimulation using a multisite stimulating electrode. It is theorized that the site size, the presence or absence of a probe shank between the sites, and the encapsulating tissue may affect the current path between the sites and that changes in this path can be detected by measuring electrical characteristics. Several electrical parameters are monitored. These include bipolar and monopolar impedance, bipolar and monopolar access resistance, anodic voltage, cathodic voltage, and charge storage. These measurements will provide information about the condition of the tissue and the electrode sites.

The experimental protocol will be reviewed briefly here. A chronic stimulating electrode is implanted in the occipital lobe of an adult guinea pig. Different probe designs were used in the two experiments. One was an eight-site four-shank device with site sizes of 400, 800, 1200, and 1600μm^2. Site pairs of the same size were grouped on a shank. The other probe had three shanks and six 1000μm^2 sites. After a 10 day rest period, the stimulation protocol began. Each bipolar pair was stimulated for 4 hours a day for five days. The stimulus waveform was a biphasic pulse of 50μA magnitude, 0.1 msec/phase duration, and 250Hz rate. A 0.6V bias with respect to the reference was placed on the sites in between pulses to obtain better charge transfer as explained in the previous report.

The experimental conditions for the two experiments to be discussed are summarized in the table below.

Experiment 1	**Experiment 2**
Site Size 1600 μm^2	Site Size 1000 μm^2
Sites of bipolar pair on same shank.	Sites of bipolar pair on different shanks.

Plots of impedance, access resistance, anodic voltage and cathodic voltage are shown below for both experiments (Figs. 1-8 are for experiment 1 and Figs. 9-16 are for experiment 2). Impedance data was acquired using a 1kHz sinusoidal, 10μA current signal. The access resistance was calculated by dividing the initial voltage drop (in response to a 50μA current pulse) by the initial current. Although most of the access resistance is due to current flow through tissue near the site, the bipolar current path will concentrate current between the two sites and may result in a different resistance than the sum of the two monopolar resistances. The difference in impedance and access resistance (Figs. 3 and 6 for experiment 1 and Figs. 11 and 14 for experiment 2) for bipolar vs. monopolar stimulation was calculated as the bipolar impedance or resistance minus the sum of monopolar measurements for each site. A positive value indicates that the bipolar, site-to-site current path has a higher resistance than the sum of the two monopolar site-to-ground paths disregarding a correction for the distant electrode. Changes in this difference measurement may indicate a change in the tissue between the sites or in the current path. The anodic and cathodic voltages (Figs. 7 and 8 for experiment 1 and Figs. 15 and 16 for experiment 2) were calculated by taking the maximum voltage developed due to an anodic/cathodic current pulse and subtracting off the voltage drop due to access resistance. The source is the site which receives a cathodic first, biphasic pulse. The magnitude of the pulse was 50μA and the duration was 0.1 msec/phase. The sink receives a pulse of equal magnitude but opposite polarity.

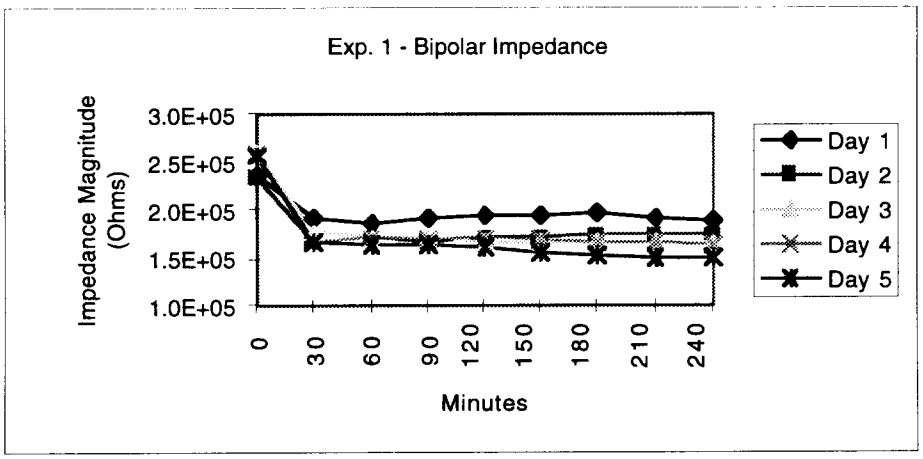

Fig. 1: Bipolar impedance at 1kHz, site size 1600μm^2.

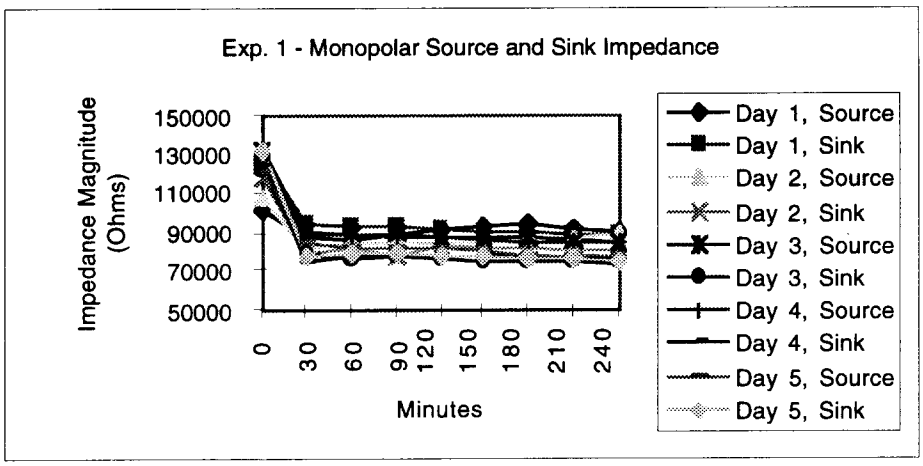

Fig. 2: Monopolar impedance at 1kHz, site size 1600 μm^2.

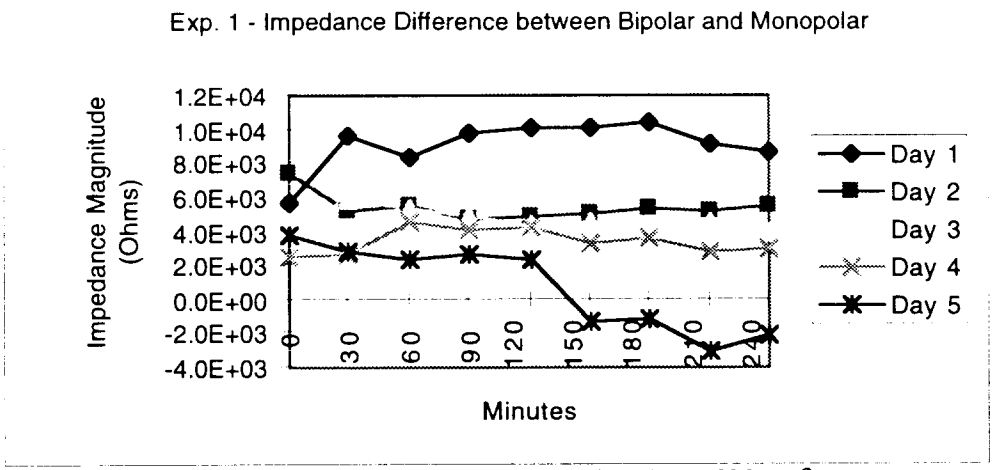

Fig. 3: Impedance Difference, site size 1600μm^2.

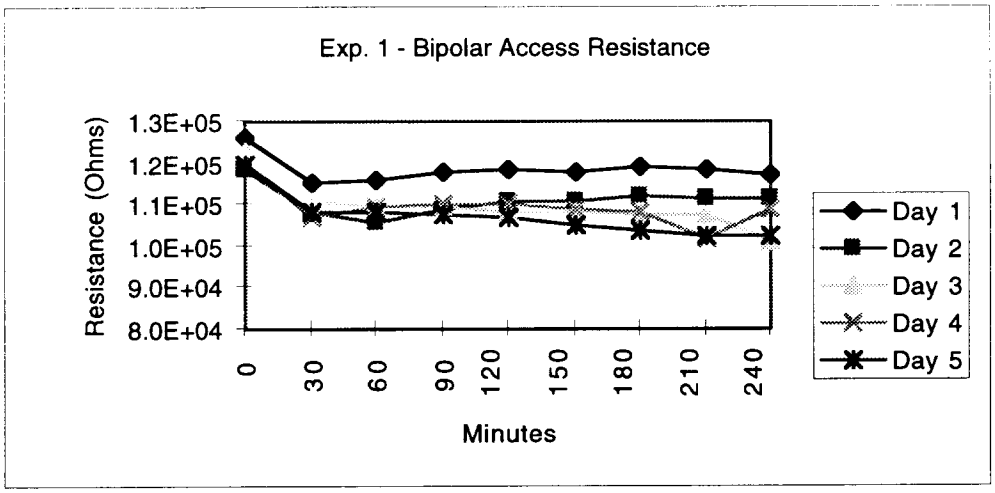

Fig. 4: Bipolar Access Resistance, site size 1600μm^2.

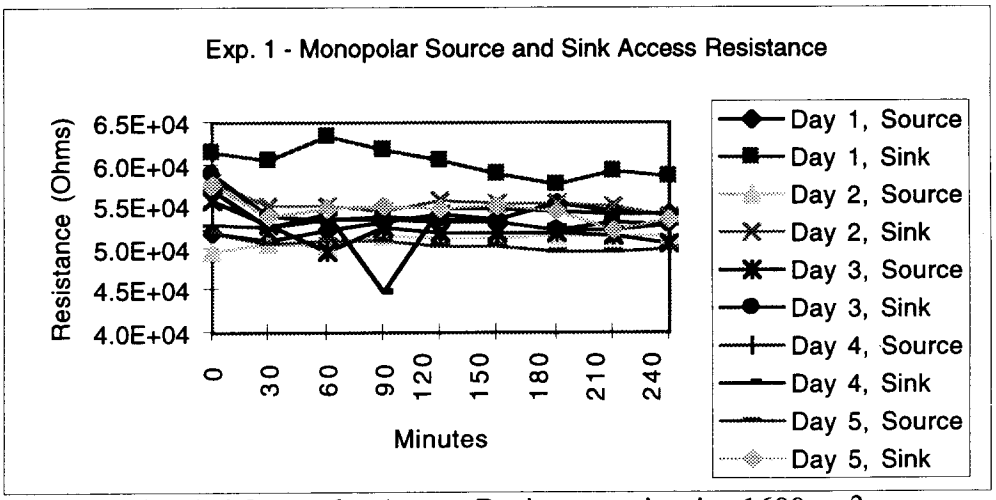

Fig. 5: Monopolar Access Resistance, site size 1600μm^2.

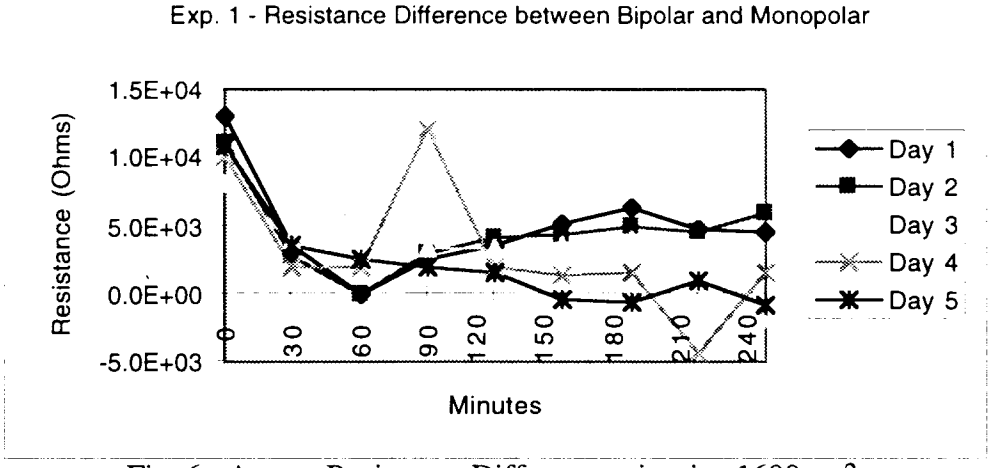

Fig. 6: Access Resistance Difference, site size 1600μm^2.

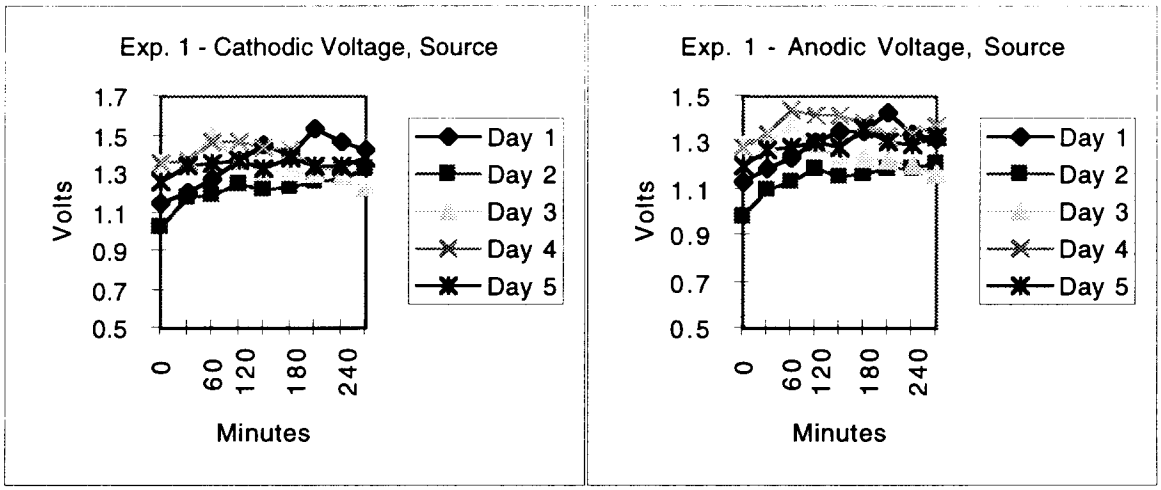

Fig. 7: Cathodic and Anodic Voltage for Source, site size 1600μm^2.

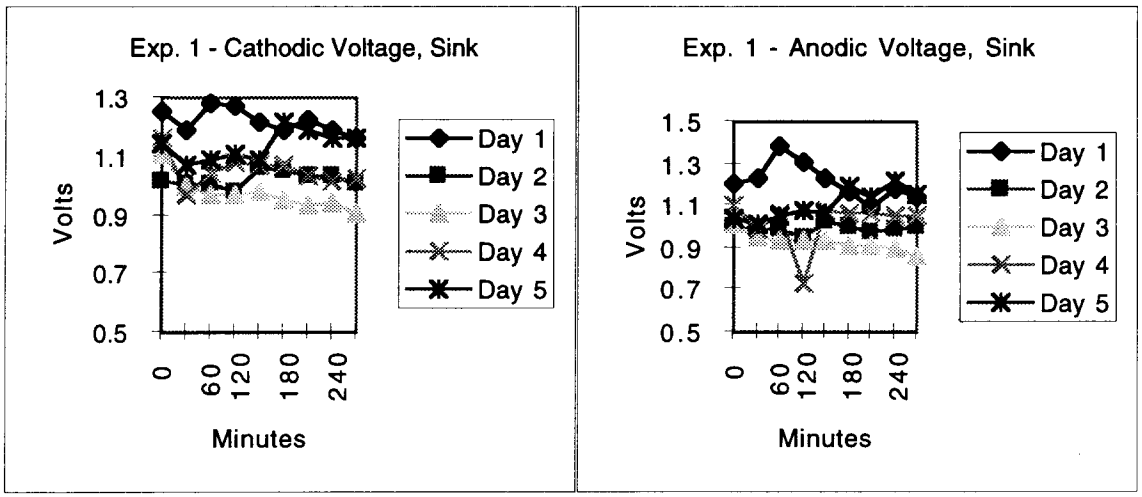

Fig. 8: Cathodic and Anodic Voltage for Sink, site size 1600μm^2.

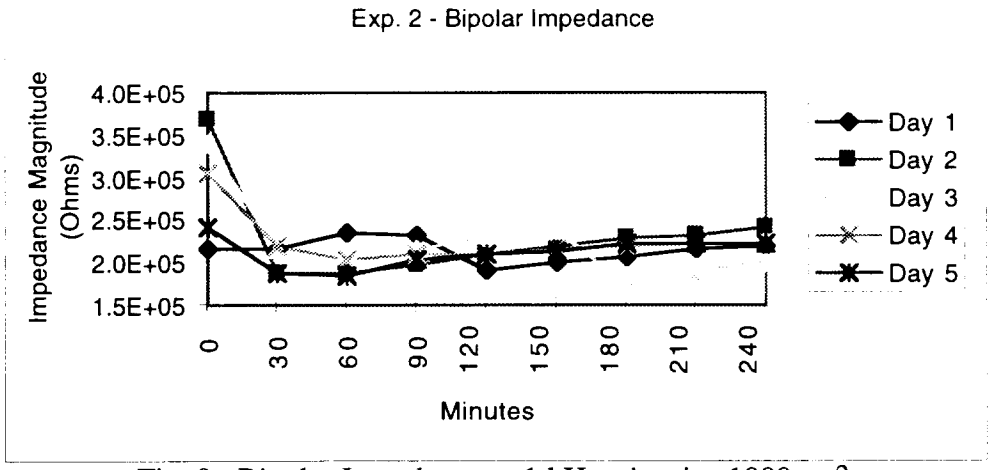

Fig. 9: Bipolar Impedance at 1 kHz, site size 1000µm^2.

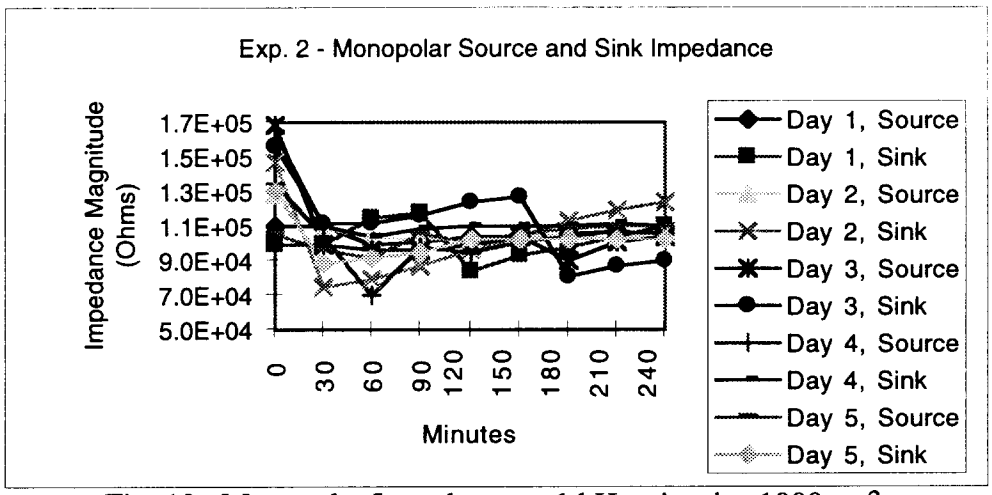

Fig. 10: Monopolar Impedance at 1 kHz, site size 1000µm^2.

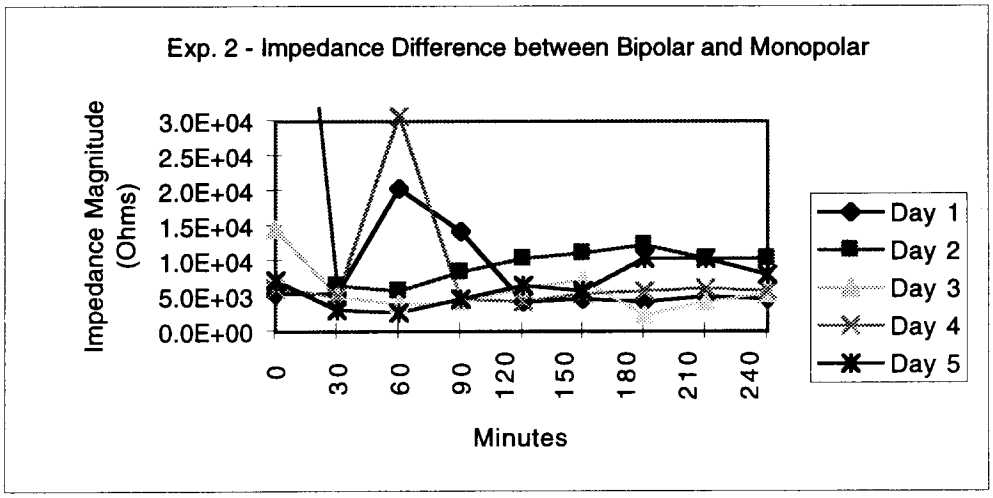

Fig. 11: Impedance Difference, site size 1000µm^2.

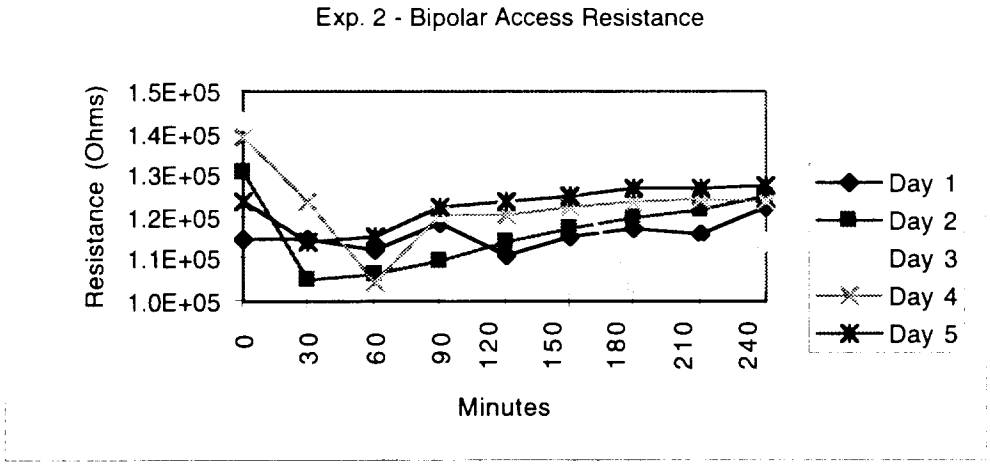

Fig. 12: Bipolar Access Resistance, site size 1000μm^2.

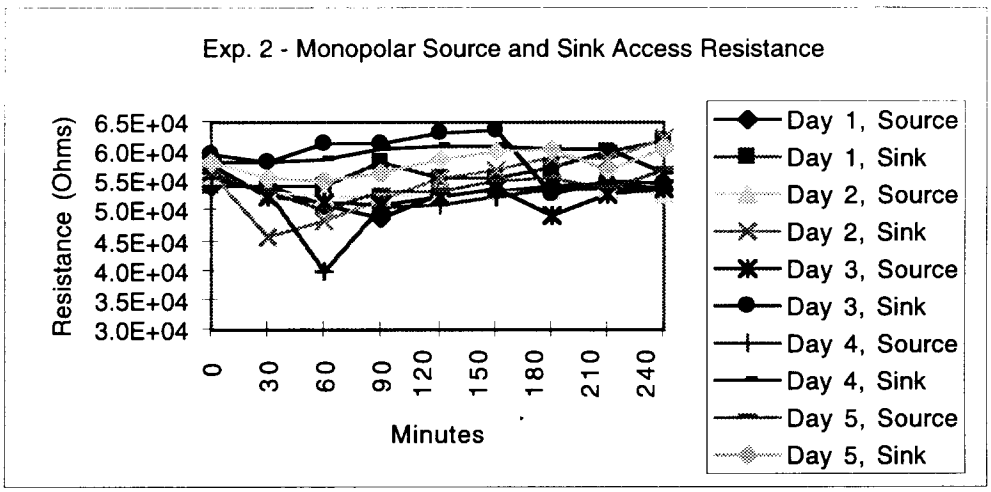

Fig. 13: Monopolar Access Resistance, site size 1000μm^2.

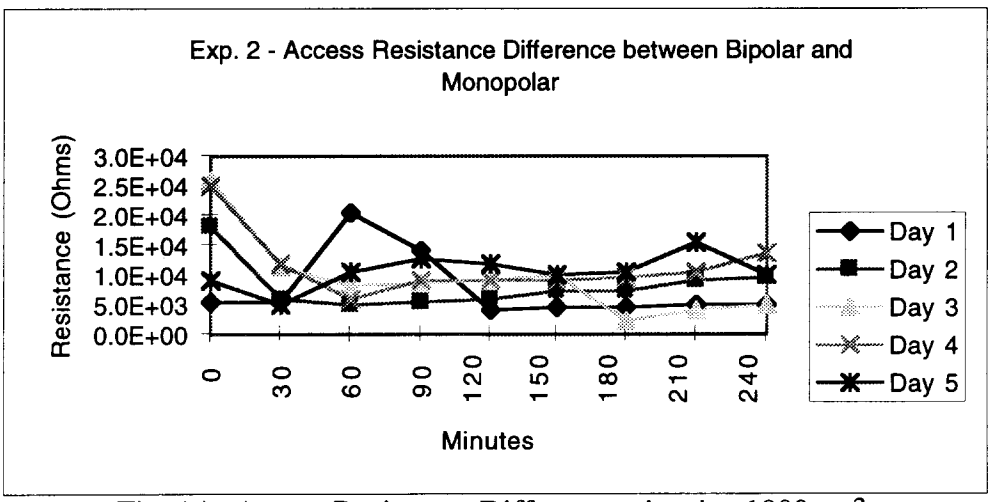

Fig. 14: Access Resistance Difference, site size 1000μm^2.

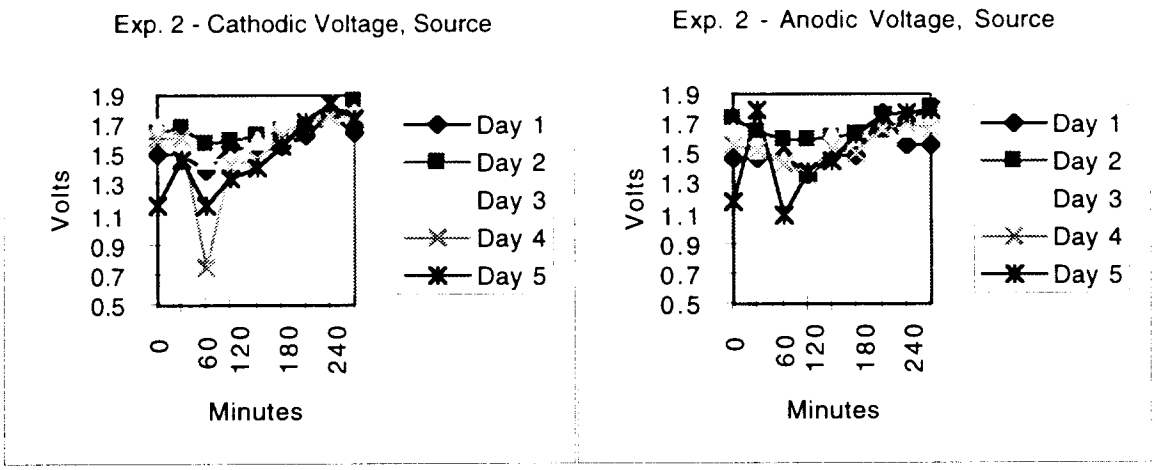

Fig. 15: Cathodic and Anodic Voltage for Source, site size 1000μm^2.

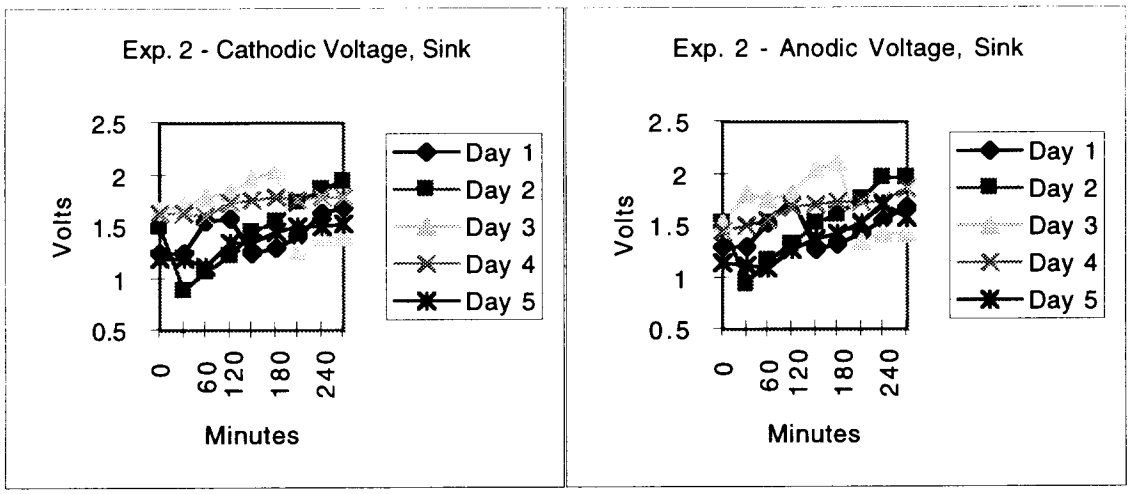

Fig. 16: Cathodic and Anodic Voltage for Sink, site size 1000μm^2.

Overall, these data show that the electrical parameters of the electrode-tissue system were fairly constant over a week of stimulation for both along shank and between shank stimulation. However, some trends were evident and merit further consideration. These will be discussed below.

The experiment 1 results show parameters recorded during along shank stimulation. The bipolar impedance in experiment 1 declined steadily from day to day throughout the week (Fig. 1). However, the monopolar impedances showed only a slight decrease (Fig. 2). As the week progressed, the bipolar current path went from having a higher resistance than the sum of the monopolar paths, to having a lower resistance (Fig. 3). The access resistance shows this same result (Figs. 5-6). Since the monopolar impedances do not change much, the tissue near the site (primarily responsible for the monopolar resistance) is probably not changing. The change in bipolar impedance and access resistance may be attributable to change in tissue resistivity between the sites or to the formation of an alternate current path (e.g., fluid near the shank inside the encapsulation). Experiment 2 used between-shank stimulation. No monotonic decline in

impedance is evident (Figs. 9-14). Between-shank stimulation would force the current to flow through tissue.

Other observations can be made. The impedance, access resistance, cathodic voltage, and anodic voltage values are generally greater for the second experiment. This is to be expected since the second test used smaller site sizes to stimulate. Both experiments showed a rapid decline in impedance after pulsing started. Separate tests showed that this change occurred in the first few minutes of pulsing. Of some concern are the numbers for cathodic and anodic voltage (Figs. 7,8,15,16). This is the potential that is being developed across the interface. Conventional wisdom places the water window at roughly ± 1.0V. These numbers regularly exceed those limits. Yet, the oxide appeared stable and seemed unaffected if gassing did indeed occur. The impedances didn't increase greatly. *In vivo* CV tests showed consistent charge storage throughout the week (hardware and data collection problems limited the amount of CV data that was saved, but the results were observed during testing). Tissue histology may tell more and is being undertaken on the tissue resulting from these experiments.

From the CV data that was taken, several observations can be made. First, the shift in the water window mentioned in the last report was evident in one of the two experiments completed this quarter. This shift occurs after pulsing and can be seen as high current flow (gassing) in a CV curve at a voltage where previously current flow was moderate (no gassing) (Figs. 18, 19). Also, by comparing the *in vitro* and *in vivo* CV curves, one can see that the charge storage capacity of the electrode is reduced *in vivo*. The low voltage range of the CV curve corresponds to the current charging the double layer. No Faradaic reactions are occurring at these voltages. The current flowing in this region is related to the capacitance of the double layer by

$$C_{dl} = I\frac{dV}{dt}$$

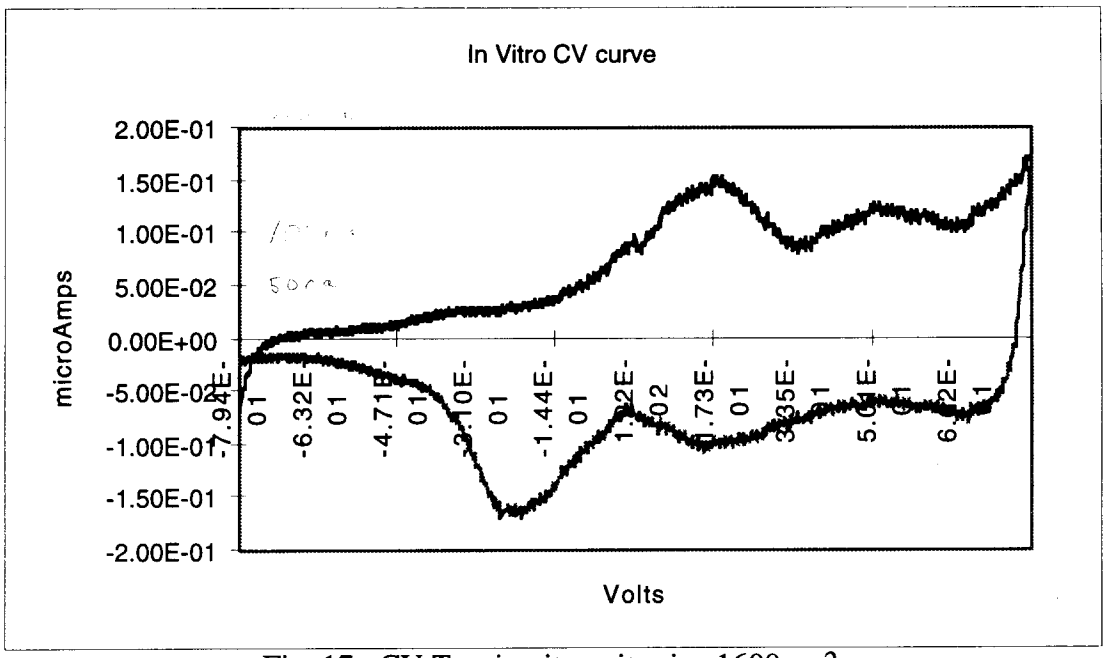

Fig. 17: CV Test in vitro, site size 1600μm^2.

The dV/dt term is the change in voltage across the double layer. When using a ramp wave, this is a constant term, so the current is proportional to the capacitance. In Fig. 17, an *in vitro* CV curve shows an activated site, while Figs. 18 and 19 show this site *in vivo*. The overall charge storage (related to the current flow) is lower in the *in vivo* CVs. However, the double layer capacitance is the same. That is, in the low voltage regions the current flow is the same for both *in vivo* and *in vitro*. The difference in charge storage comes from the decreased efficiency of the Faradaic reactions *in vivo*. The cause for this decrease could be found in the concentration of reactants at the interface or the accessibility of the interface to diffusing ions.

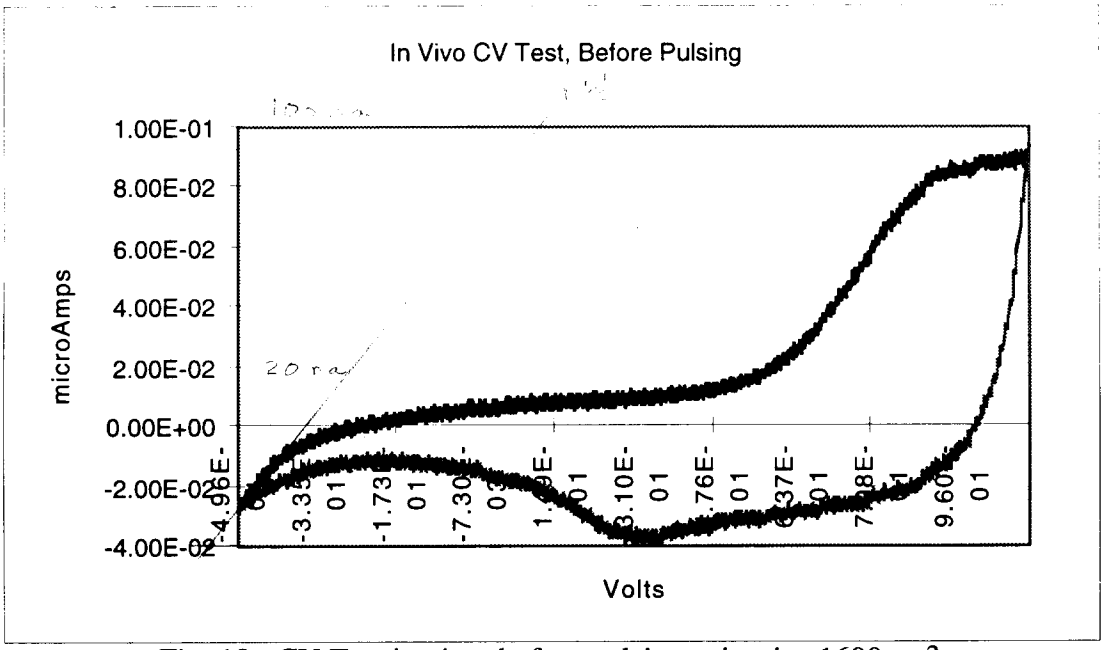

Fig. 18: CV Test in vivo, before pulsing, site size 1600μm^2.

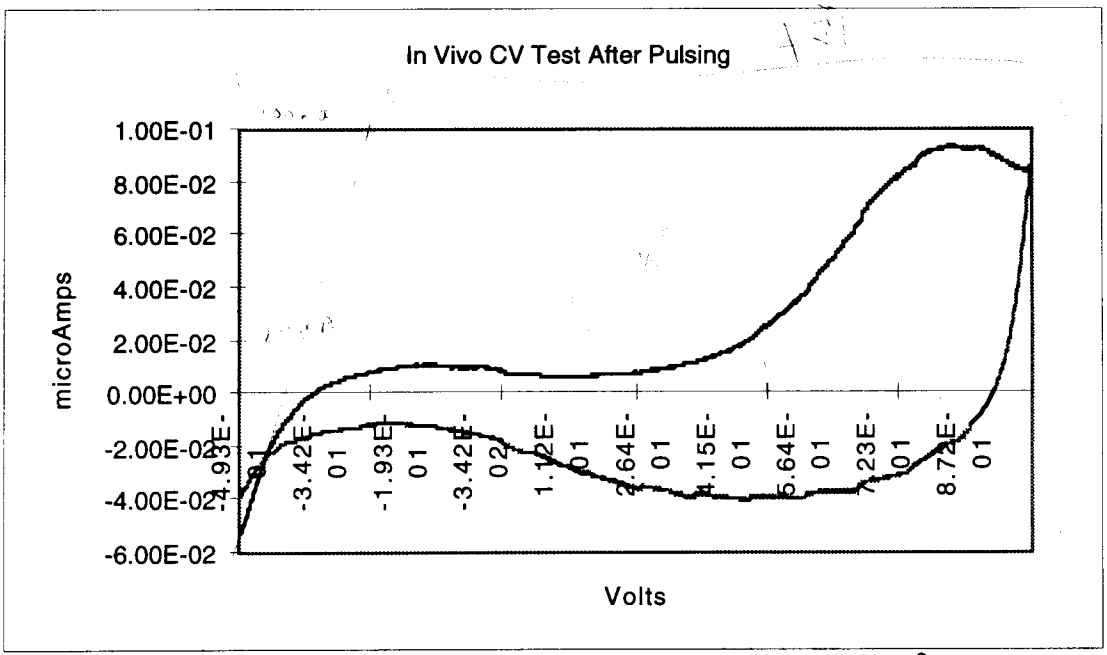

Fig. 19: CV Test in vivo, after pulsing, site size 1600μm^2.

Some calculations can be made from these data. The difference between the current for the positive and negative sweeps is roughly 20μA for all three plots shown. The ramp speed is 0.5V/sec, which results in a C_{dl} of about 5nF. In theory, the double layer has a capacitance of 20μF/cm^2. For an unactivated 1600μm^2 site, this results in a capacitance of 320pF. Activation can increase the capacitance by increasing the surface area.

A long term *in vitro* pulse experiment was begun. This test follows a similar stimulation protocol as the in vivo test, except that the electrode is placed in PBS. The probe used in this test was fabricated with the new metalization protocol. Pulsing is being performed to validate the adhesion of the iridium. To date, approximately 160 million pulses have been applied to the electrode sites. After an initial drop in impedance during the first day of testing, no fluctuations have been seen. Bipolar impedance for three separate days are plotted below (Fig. 20). This test will be continued through the next quarter.

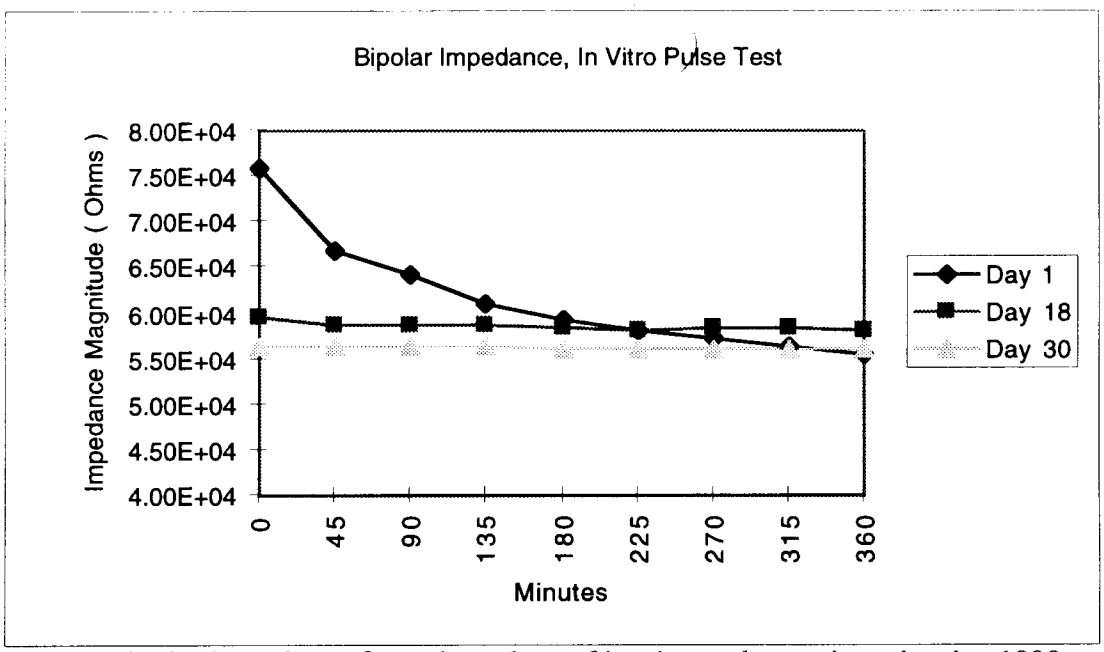

Fig. 20: Bipolar impedance from three days of in-vitro pulse testing, site size 1000μm^2.

During the next quarter, we hope to report on histology from the animal experiments discussed above. We will complete several more animals studies and will continue pulse testing experiments during this period.

4. External Interface for Active Stimulating Probes

In this area, the goal for the last few months has been to work towards the fabrication of external electronic interface systems based upon the prototype system which was assembled and validated. The circuit design, which previously existed only as a paper-and-pencil schematic, was entered into a CAD system in anticipation of the remaining steps of the process: PCB layout, routing, and manufacture. These last three steps could not be performed, however, since the necessary software for PCB design did

not arrive until recently. The PCB design is the next step in the process. An effort will be made to complete this project as quickly as possible.

In support of experiments using active stimulation probes, a program module was developed that generated repetitive bipolar, biphasic pulses at real-time speeds (up to 4MHz). Previously, the speed of stimulation was limited by the external software, which was only designed for testing and prototyping, not real-time stimulation. This program module was integrated into the existing character-based interface program. Eventually, the graphics-based interface program that is currently under development will assume this function.

5. Development of Active Stimulating Probes

During the past quarter, work on active stimulating probes focused on realizing usable probes of all three designs: monopolar, bipolar and multipolar (STIM-1b, STIM-1a, and STIM-2). More probes were completed, carrying out the final etch step on wafers previously fabricated. We expect to be able to utilize the STIM-2 probes (the multipolar 64-site probes) from the last fabrication run in spite of the lower than expected sink current on some of these devices as noted in the past report. The monopolar probe (STIM-1b) and the bipolar probe (STIM-1a) have been utilized during the present quarter in in-vivo experiments and in-vitro characterization, respectively. As we test these devices, we are accumulating a list of needed changes for the next mask iteration so that we can arrive at devices suitable for long-term in-vivo evaluation during the coming year.

STIM-1B

STIM-1b is the simplest version of the active stimulating probes. The probe uses an input clock to drive an on-chip four-bit counter to enter a serial address and select one of sixteen sites. The selected site is connected to the analog data input pad through a pass transistor. The counter is initially reset to the first site by strobing the clock line negative. This probe is a monopolar device which simply acts to steer an externally-generated current to the appropriate site. The functionality of this device is dependent mainly on the correct operation of the digital logic circuitry for selecting the correct site for current delivery. The lack of any analog circuitry makes the design very robust with regard to its dependence on process parameters.

The completed STIM-1b probes were found to function exceptionally well in-vitro. Figure 21 demonstrates that STIM-1b is capable of functioning properly even with a very marginal 10MHz clock (upper trace). The data signal is a 1.6μsec/phase biphasic voltage pulse (middle trace). For ease of testing, a ±5V voltage pulse was used as the data signal rather than a current source. The lower trace is the voltage generated across a 1MΩ resistor in series with the saline bath in which the probe was being driven. Hence, the current sourced and sunk is displayed. For this test, the same channel was selected on subsequent pulses; however, alternate channels could also be selected with correct operation still being obtained at the 10MHz input address clock rate.

The STIM-1b probes have also been used for in-vivo experimentation. The results of the in-vivo testing have demonstrated the potential of these probes, although we have not yet been able to obtain all of the results that we would like. The in-vivo testing performed during the past quarter involved first placing a silicon recording probe in the inferior colliculus (IC) of a guinea pig and verifying its ability to record the response to an auditory stimulus. The recording electrode was then cemented to the skull with dental

acrylic in order to fix its position. The cochlear nucleus (CN) was then exposed and a STIM-1b probe was inserted for stimulation. The CN was presented with a 100Hz sine wave stimulus for 100mSec (10 sinusoidal cycles). The stimulus was presented 200 times and the number of spikes recorded from the IC were summed into 100µsec bins referenced to the onset of each stimulus in order to observe the response versus time.

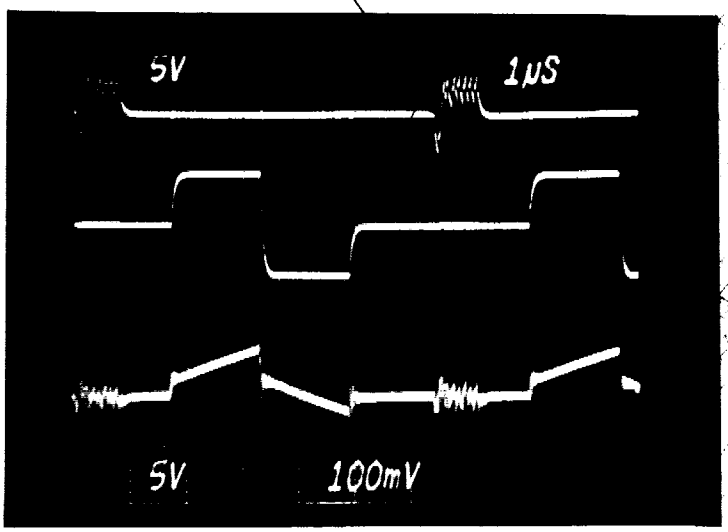

Fig. 21: STIM-1b operating with a 10MHz input clock (upper trace) and being driven by a ±5V 1.6µsec/phase biphasic voltage pulse (middle trace). The probe output (lower trace) is the voltage across a 1MΩ resistor in series with the saline bath.

The intent of this experiment was to be able to show that stimulation of certain sites would produce a response (change in the spike count) at a give recording site while stimulation at other sites would not result in a response. We have indeed observed such behavior, but due to an intermittently saturating recording amplifier in our experimental setup, acquiring clean records has been a problem. Figures 22 and 23 are examples of the records obtained thus far with and without stimulation, respectively. With the stimulus applied (Fig. 22), units are clearly being driven in synchrony with the stimulus current maxima as should be expected, i.e., units are firing in conjunction with the maximum sourcing and sinking currents at about 5msec intervals. It is also interesting that in virtually every case, the negative half cycle is more effective in stimulation than the positive half cycle. When the stimulus is not present, there is no such synchronous activity. When the stimulating site was changed to another site, the driven activity was altered but due to external instrumentation problems, proper documentation was not obtained. The experiment will be repeated during the coming month.

STIM-1A

STIM-1a is a first generation probe with the capability for on-chip bipolar current delivery. The probe can source and sink current by selecting any two of its sixteen 450µm^2 sites, one as the current source and the other as the current sink, by clocking in a fifteen bit data word and latching it with a negative clock strobe. The first four bits

specify the site address of the current sink electrode, the next four bits specify the site address of the current source electrode and the last seven bits specify the amplitude of the current to be driven, which can be as high as 254μA with a 2μA resolution.

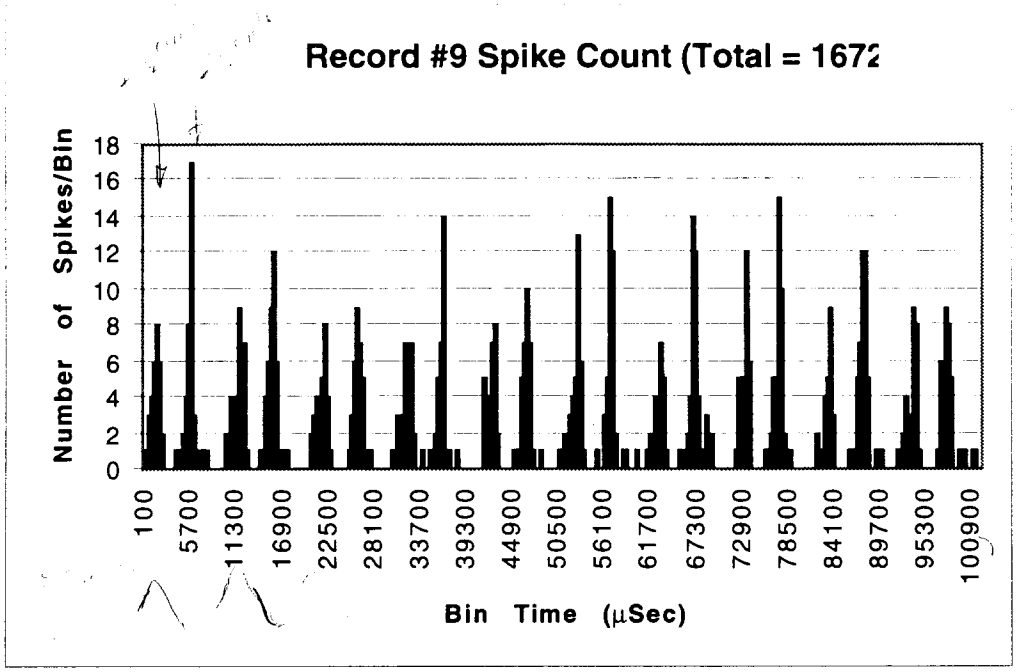

Fig. 22: Histogram of spikes recorded with a silicon recording probe from IC during stimulation in the CN with a multichannel STIM-1b, where each bin is a 100μsec time slice.

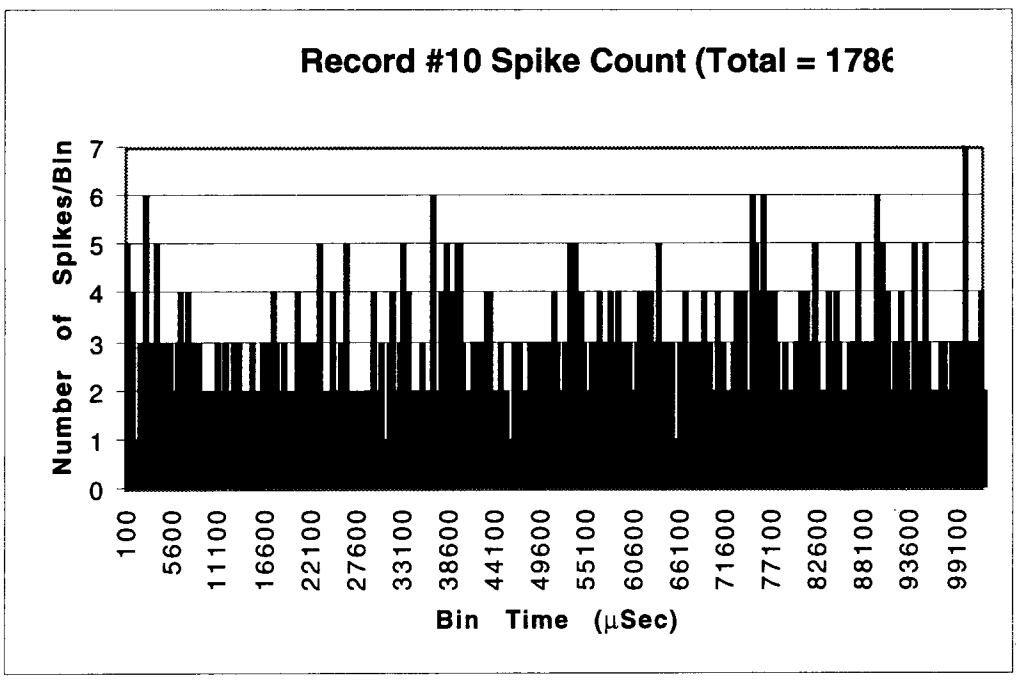

Fig. 23: Histogram of spikes recorded with a silicon recording probe from IC without any stimulation, where each bin is a 100μsec time slice.

Figure 24 demonstrates the functionality of STIM-1a before being separated from the wafer when operating with a 2.6MHz clock. The STIM-1a probes that have been etched out in the past quarter have been tested in-vitro and appear to be functioning close to specifications. Figure 25 demonstrates STIM-1a driving current in a saline bath while operating from a 3.3MHz clock signal (upper trace) with sites 0 and 12 alternating to source and sink maximum current. Site 0 is at the tip of a shank whereas site 12 is at the top end of a shank. This allows placing only one of the sites in saline to observe its current alone, site 0 (lower trace). Otherwise, the net current put into the solution would be zero. The upper limit on the speed appears to be due to the inability of the external electronics to pull the clock line low enough at high speed when immediately surrounded by positive pulses. Increasing the negative supply voltage improved the speed of the circuit as the magnitude of the negative strobe increased, as expected. This problem was not present in the case of STIM-1b because the clocking scheme does not cause such severe degradation of the negative pulse. Figure 26 shows an SEM view of the back end of a recently completed STIM-1a probe.

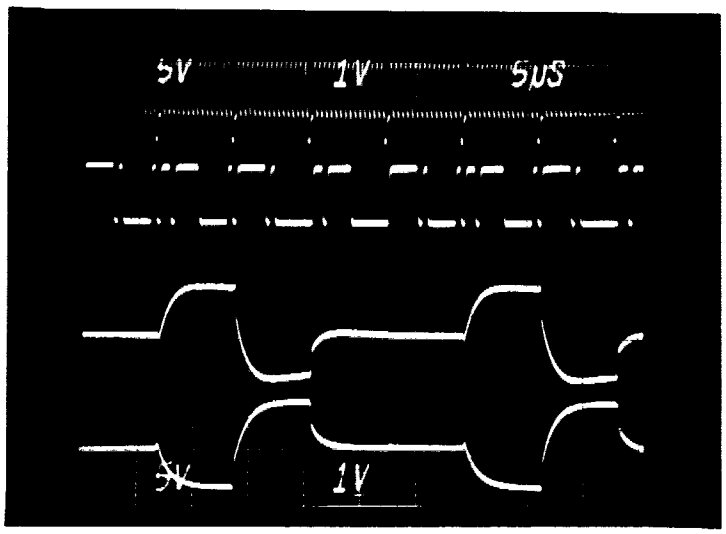

Fig. 24: STIM-1a (on wafer) operating with a 2.6MHz clock driving biphasic current into a resistive load.

In order to use the STIM-1a probes it is necessary to characterize the current that the probe actually delivers to the tissue. This is somewhat more complicated on this probe than on the monopolar or multipolar probes because the total current delivered from the bipolar sites should be zero. One possible characterization method is to measure the current delivered by the power supplies. This will be somewhat higher than the true output current due to the biasing currents flowing in the probe. Figures 27 and 28 show plots of the current corresponding to each bit of the output DAC. The plots demonstrate that the current in the positive power supply does indeed track the output sourcing current closely with a fairly constant offset of about 20μA. However, in the case of the negative sink current, the characteristic is nonlinear. The sink current tracks the negative supply current and is close to the design value up to about 80μA. Above this point there is a sharp break in both curves and the current becomes a much weaker function of the DAC setting. The offset (bias) current is still about 20μA as expected. We are unsure of the origin of this nonlinearity but it is being investigated. It is characteristic of saturation in

the output device and may be due to that or to a problem in the current mirror circuit that drives the output stage of the DAC. This mirror circuit should ensure that the sourcing and sinking currents are matched to better than one percent for the two bipolar sites, and it is very important that it does. On the monopolar and multipolar probes, source/sink mismatches can be corrected by independently correcting the DAC codes for the two currents; however, on the bipolar probe they are generated simultaneously from the same input code and this correction cannot be done. We expect to understand the source of the high-sink-current nonlinearity during the coming term and whether it is a problem due to process parameters, test conditions, or circuit design. In any case, it will be corrected on the next process run.

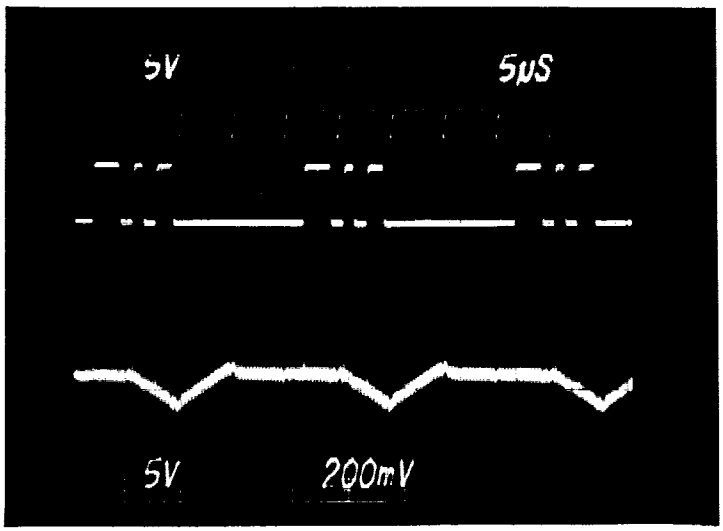

Fig. 25: STIM-1a driving current in saline from a 3.3MHz clock (upper trace), sinking and sourcing maximum current (middle trace, data) on sites 0 and 12, respectively. Only site 0 is in solution. The probe output current (lower trace) is the shown as the voltage developed across a 1MΩ resistor in series with the solution.

STIM-2

STIM-2 significantly extends the capabilities of the first generation probes in many areas. STIM-2 incorporates flexible interconnects, which allow the rear circuit-containing portion of the probe to be folded flat against the cortical surface to reduce the probe height above the cortical surface in an implant; new circuitry for power and area reduction while increasing functionality; a front end-selector which allows 8 of 64 sites to be driven simultaneously, thereby implementing electronic site positioning; and compatibility with use in a multi-probe three-dimensional array.

In an attempt to utilize the STIM-2 probes obtained from the most recent fabrication run for in-vivo tests, we have explored the possibility of improving the current sinking ability of the probes by varying the supply voltages. By increasing the negative supply V_{ss} to -5.8V, a maximum sink current (1111111) of -66μA was obtained as shown in Fig. 29. The sourcing current matches this level at (0001011). The increase in V_{SS}, imbalancing the supplies, reduces maximum operating frequency, although the resulting speed is still sufficient for initial in-vivo testing (50kHz). The maximum operating frequency can be doubled by also increasing V_{DD}. By adjusting both supply voltages

(V_{DD} = 5.80V, V_{SS} = -5.95V), the probe was able to run with a clock frequency of 400kHz (the minimum frequency at which the custom external interface electronics can currently run) and still sink up to 66μA of current, even though the negative current pulse turn on is still rather slow. We are planning to slow the frequency (by changing the crystal) of the external interface electronics to the point where we can obtain a minimum pulse width of 100μsec and use the probe for standard biphasic stimulation. The cause of the weak pull-down is still under study so it can be corrected on the next process iteration.

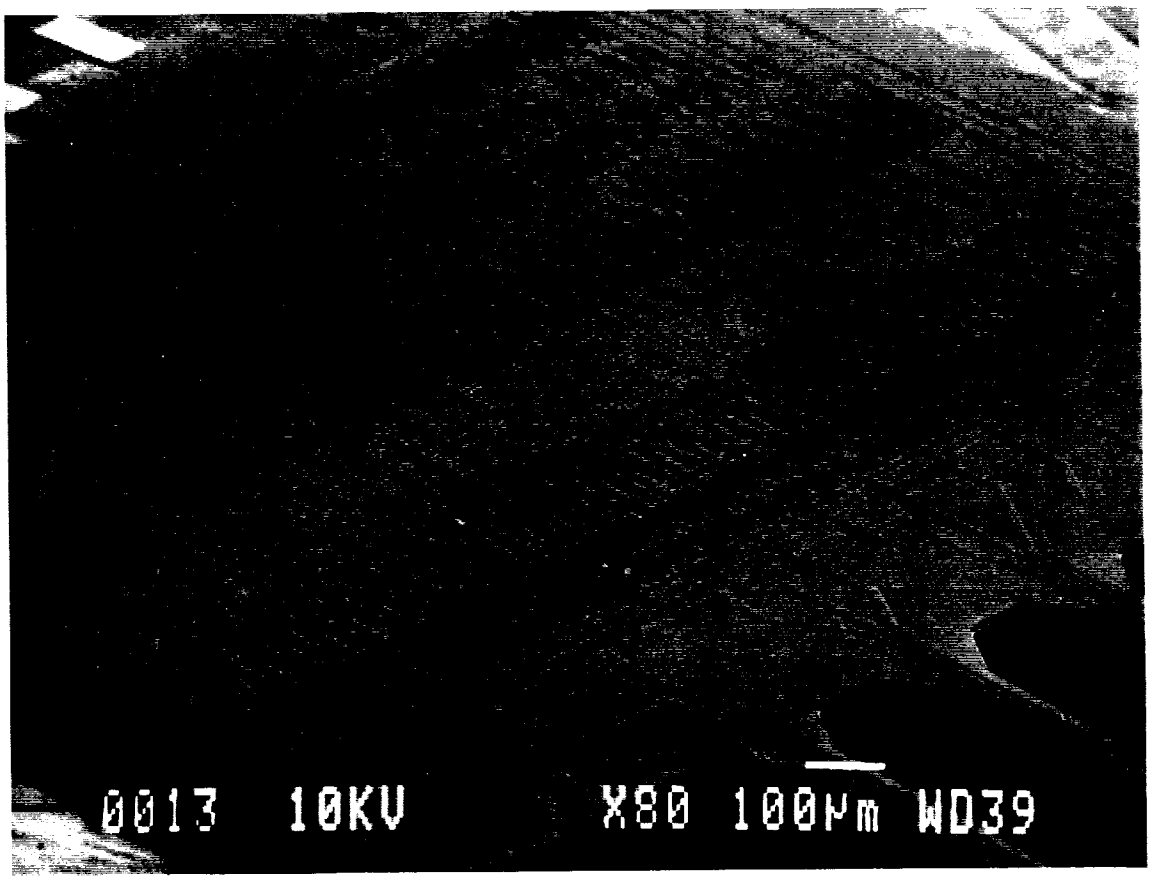

Fig. 26: SEM view of the circuitry of a STIM-1a active probe realized during the past term.

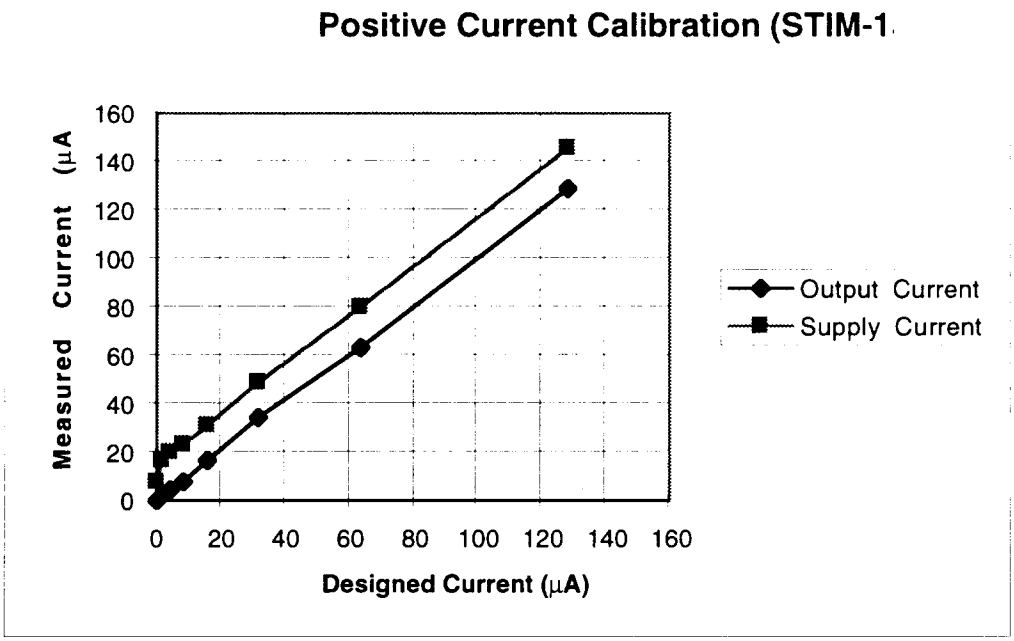

Fig. 27: Comparison of the output sourcing current and the positive supply current versus the designed current delivery (DAC code) for current sourcing in STIM-1a.

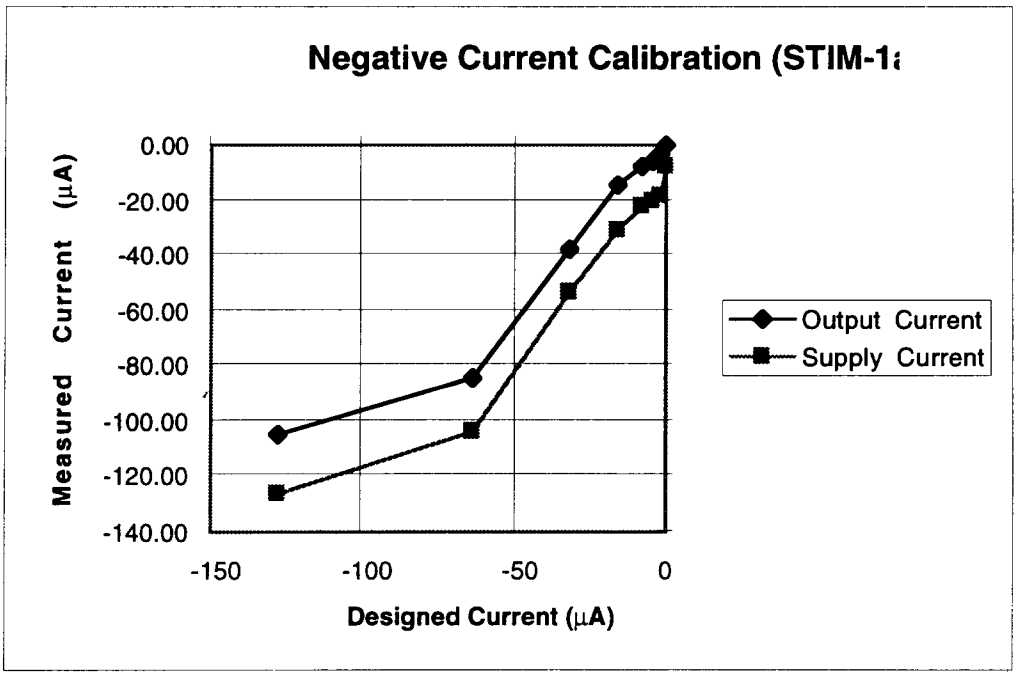

Fig. 28: Comparison of the output sink current and the negative supply current versus designed current delivery (DAC code) for current sinking in STIM-1a.

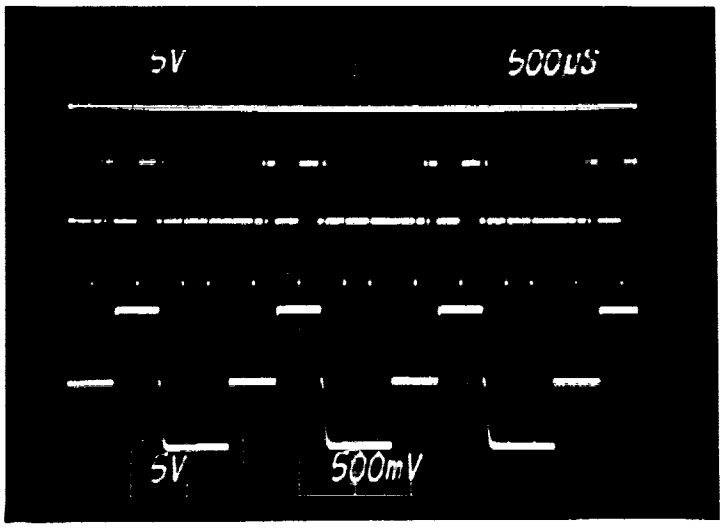

Fig. 29: The output of STIM-2 (lower trace) with the negative supply voltage increased to -5.8V. The maximum current sink is increased to -66μA at the cost of reduced maximum operating frequency.

During the coming quarter, we plan to complete the fabrication of more of the active probes (all designs) so that we can make use of them in-vivo. As we identify problems we will explore their sources so that they can be corrected on the next process run later this fall. Actual use in in-vivo experiments will also help in evaluating the current addressing and/or mode protocols so that they can be changed if necessary.

5. Conclusions

During the past quarter, work under this contract has been peformed in several areas. We have continued to fabricate passive probes for both internal and external users and are currently in the process of completing probes from four different mask sets. We are using the new site techniques described in the last quarterly report and have seen no further evidence of iridium adhesion problems. During the quarter, a number of chronic stimulation experiments were also completed. Electrode and tissue impedance, access resistance, and cyclic voltammetry data were taken throughout a week of stimulation on animals for two different current flow conditions. The chronic stimulating electrodes were implanted in the occipital lobe of an adult guinea pig. After a 10 day rest period, the stimulation protocol began. Site sizes of 1600μm^2 and 1000μm^2 were used. Each bipolar pair was stimulated for 4 hours a day for five days. The stimulus waveform was a biphasic pulse of 50μA magnitude, 0.1 msec/phase duration, and 250Hz rate. A 0.6V bias with respect to the reference was placed on the sites in between pulses. The electrical parameters of the electrode tissue system remained fairly constant during the measurement period for both along-shank and between-shank stimulation, indicating no significant changes in either the electrode properties or the tissue near the electrode as the result of stimulation. In addition to these tests, a long-term in-vitro pulse experiment was begun in PBS with parameters similar to those used in-vivo. The probe used in this test

was fabricated with the new metalization protocol. To date, approximately 160 million pulses have been applied to the electrode sites. After an initial drop in impedance during the first day of testing, no significant subsequent changes have been seen.

Additional tests have been performed in-vitro and in-vivo using active probes realized from the most recent fabrication run. The monopolar probe, STIM-1b, functions well at frequencies up to 10MHz and has been used in additional experiments to stimulate in cochlear nucleus of the guinea pig while a silicon recording probe monitored the resulting driven single-unit activity in inferior colliculus (IC). As the site of stimulation was changed over the active probe, the patterns of single-unit activity in the IC have been seen to change accordingly. While preliminary in nature, these experiments mark the first successful use of an active probe in tissue. STIM-1a, an active bipolar probe, has also been characterized further in-vitro. The background bias current on both the positive and negative supplies is about 20μA, which is very close to the level expected. The current sourced by this probe is a linear function of the DAC setting over the full 0 to 127μA output range as expected. However, the negative sink current is linear only up to about 80μA, above which it has a weaker dependence on the DAC setting. The reason for this nonlinearity is being investigated but the problem should not preclude use of the probe at lower current levels. A weakness in the ability of STIM-2, the multipolar probe, to sink high currents has also been observed as noted in the previous report. By adjusting the supply voltages, however, this device can sink currents of over 60μA at frequencies of up to 400kHz. This is high enough to allow the use of STIM-2 in many in-vivo experiments, where additional experience using the probe will be gained during coming months. Needed changes will then be made to the probe design so that all observed problems can be corrected in a single design/process iteration later this year.